Scaling cluster blast wave physics to high energies, relativistic intensities and ultra high mach numbers

M. Hohenberger, J. Lazarus, R. E. Carley, H. W. Doyle and R. A. Smith
Laser Consortium, The Blackett Laboratory, Imperial College London, Prince Consort Road, SW7 2BW, UK

D. R. Symes, R. J. Clarke and M. M. Notley
Central Laser Facility, STFC, Rutherford Appleton Laboratory, HSIC, Didcot, Oxon OX11 0QX, UK

A. S. Moore and E. T. Gumbrell
AWE plc, Aldermaston, Reading RG7 4PR, UK

Contact | M.Hohenberger@Imperial.ac.uk

Introduction

The rapid development of short-pulse, high-power laser systems over the last decade has made it possible to produce high-energy-density plasmas on a sub-millimeter scale. This enables the study of phenomena in the laboratory that are otherwise found only in astrophysical systems[1]. Even though laboratory and astrophysical systems differ by many orders of magnitude in both temporal and spatial scale, they are governed by the same physical processes. In fact, both scenarios can be shown to be hydrodynamically equivalent provided that characteristic dimensionless parameters such as the Mach, Reynolds and Peclet number are comparable[2]. Ultimately this enables the systematic study of astrophysical plasmas using scaled laboratory analogues driven by high-intensity lasers, provided that suitable initial conditions can be reached.

From high-resolution images of astrophysical nebulae and supernova remnants (SNR) such as SN 1987A, it can be seen that rather than being smooth, these systems generally exhibit an intricate structure full of turbulence and knotted regions[3]. Formation of these complex structures is thought to be driven by strong shocks and blast waves, highlighting the importance of the study of these phenomena for laboratory astrophysics and, more generally, for high energy density plasma physics[1]. Studying instabilities and overstabilities in SNR-like structures on a laboratory scale using high intensity ($\geq 10^{16}$ Wcm^{-2}) lasers can be elegantly realised by utilising the unique absorption properties of clusters as a target medium[4,5].

Gas targets typically absorb <1% when irradiated with a high intensity laser, producing only relatively low temperature plasmas, while the presence of clusters in the gas has been demonstrated to increase the absorption efficiency up to ~90%[6]. This allows for a substantial deposition of energy into the target medium creating low-average-density high-temperature plasmas. We report on new investigations of energy absorption and energy transport from high-intensity laser interactions with a range of low to high Z cluster targets and far higher drive energies than previously reported. Results from smaller (few J) laser systems at Imperial College have been scaled to higher energies by two orders of magnitude and into the relativistic regime ($>10^{18}$ Wcm^{-2}) using Vulcan. Furthermore the impact of pre-ionising the ambient medium surrounding an expanding blast wave is demonstrated using a secondary X-ray source.

Experimental details

The experiment was performed in TA West using the Vulcan Nd:Glass laser which delivered on-target energies up to 60 J in a 1.3 ps pulse with the wavelength λ=1054 nm. An f/18 parabola was used to focus the beam to a 40 μm spot resulting in a normalised vector potential of a_0 = 1.7. The focus was aligned 3 mm above the centre of a cluster source, produced by a gas jet (Parker Hannifin Corporation Series 99), modified to support cryogenic cooling of the backing gas. The gas jet was operated using an externally triggered pulse generator (IOTA ONE) with additional electromagnetic pulse suppression[7] to avoid damage from laser driven EMP. The gas nozzle was modified and elongated to allow for a larger solid angle of accessibility providing more viewing angles for a broad range of diagnostics.

The interaction was imaged with the second CPA beam available in TA West, which was spatially filtered and frequency doubled to 527 nm. Before entering the vacuum chamber, the probe beam was split into S and P polarisation with an adjustable time delay between the two. Subsequently it was divided into three individually timed, separate pulses providing a backlighter for interferometry and Schlieren imaging systems. This resulted in a total of six pairs of time-separated interferometric and Schlieren images all acquired on a single shot. A fourth long-pulse optical probe line was used to back-illuminate the interaction with a doubled, Q-switched Nd:YAG laser (Continuum Surelight) with its nominal pulse duration of 5 ns stretched to ~40 ns using an etalon array. The stretched pulse was used to image the interaction onto a streak camera (Hamamatsu C5680) providing a full blast wave trajectory on a single shot basis[5].

Four Si PIN diodes filtered with thin metal foils were positioned inside the vacuum chamber at various angles to the laser cluster interaction to measure potential side scattering. An Andor DV420 camera was positioned above the interaction at 90° to image self-emission from the plasma. The laser energy transmitted through the target medium was measured with a large area disc calorimeter (Scientech 38-0801) positioned 125 cm behind the gas jet target and outside the vacuum chamber. The X-ray plasma emission was measured with a series of Andor back thinned X-ray CCD cameras cooled for noise reduction and filtered with a range of materials. Two of these

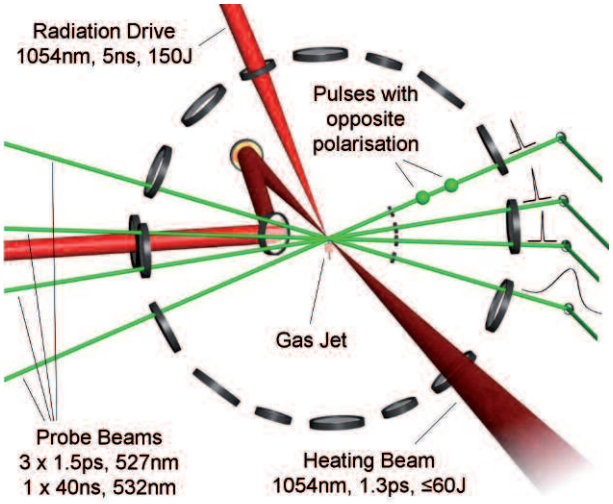

Figure 1. Schematic outline of the experimental setup. The green beams are optical backlighters providing a total of twelve snapshots of the laser cluster interaction, with pairs of Schlieren and interferometry images captured at six separate timesteps. Streaked Schlieren imaging also tracked the full plasma evolution on a single shot. An additional radiation drive was produced by focusing a long pulse beam onto a Au-target to launch X-rays and locally ionise the target medium. Diagnostics such as the Si PIN diodes and multiple X-ray cameras have been omitted for clarity.

cameras were run in single photon mode (Andor DV434 BN) and another three (Andor DV420, DV440 and DV434) imaged the spatial profile of the interaction via pin-holes. Unfortunately we could not extract temperature measurements from the single-photon cameras because even at the furthest possible distance from the interaction the high photon flux necessitated heavy filtering which ultimately dominated the camera response.

To quantify the impact of radiation and ambient gas ionisation on the plasma evolution we implemented an additional radiation drive designed to launch soft X-rays at ~50 eV into the cluster gas and locally ionise the medium. The X-rays were generated by a long pulse beam (5ns, 150J) incident onto a Au target attached to a pair of Au coated glass slides to act as a grazing incidence guiding and collimating structure. A schematic drawing of the experimental setup can be seen in figure 1.

Energy deposition in cluster media

One of the main interests in clusters as a target medium for high-energy-density plasma physics is their uniquely efficient absorption of high-intensity laser radiation. Previous studies of laser absorption in cluster media have been performed at sub-relativistic [6] ($<10^{17}$ Wcm^{-2}) as well as highly relativistic intensities [8] ($>10^{19}$ Wcm^{-2}). Initial results saw a significant increase in absorption for intensities $\geq 10^{13}$ Wcm^{-2} compared to unclustered gas, which for $I \geq 10^{14}$ Wcm^{-2} quickly rose and plateaued at about 90% indicating absorption saturation and followed by a drop in absorption for a further intensity increase. Initially this was attributed to a 'burn through' of the cluster medium by the leading edge of the laser pulse. As energy from the laser pulse is absorbed by the clusters, they start to expand on a 100-200 fs timescale, much shorter than the 2 ps pulse duration used for the experiment so that the trailing edge of the pulse is not absorbed efficiently. On the other hand, the data taken at relativistic intensities also exhibits 80-90% absorption, despite the initially observed drop. However, differences in pulse duration, laser wavelength, cluster size and pulse contrast cannot be ruled out as contributing factors.

Absorption measurements were conducted in our experiment for four different gases H_2, Ar, Kr and Xe with an average cluster radius of about 4 nm, 8 nm, 12 nm and 15 nm, respectively. The calorimeter was calibrated against a power meter with a known response. Without operating the gas jet, the calorimeter measured the full energy delivered onto the target. When the clusters were present, the calorimeter registered only the energy that had been transmitted and not absorbed or scattered by the cluster medium. Significant side-scatter would have been detected with Si PIN diodes, but no signal above the noise level was observed for any of the shots. This validates the assumption that the calorimeter registers all of the energy not absorbed by the target medium.

Figure 2 shows a plot of absorption as a function of laser intensity for all four target gases. The absorption is defined as $1\text{-}E_{out}/E_{in}$ with E_{in} being the on-target energy and E_{out} being the transmitted energy measured by the calorimeter. As can be seen, for Ar, Kr and Xe the absorption efficiency is typically above 80% and does not exhibit the initially observed drop in absorption for intensities exceeding 10^{17} Wcm^{-2}. This, in conjunction with the data presented in ref. [8], therefore underlines the potential of a cluster target medium to efficiently absorb high-intensity laser radiation spanning at least 2-3 orders of magnitude in energy. It seems likely that the reduced absorption observed in ref. [6] for higher intensities could have been caused by a laser pre-pulse. The clusters would absorb energy and start to expand under the influence of the pre-pulse, so that by the time the main pulse arrives, they are completely disassembled.

It is also clear from figure 2 that H_2 only absorbs ~50% of the energy at the intensities used here. This is in contrast to

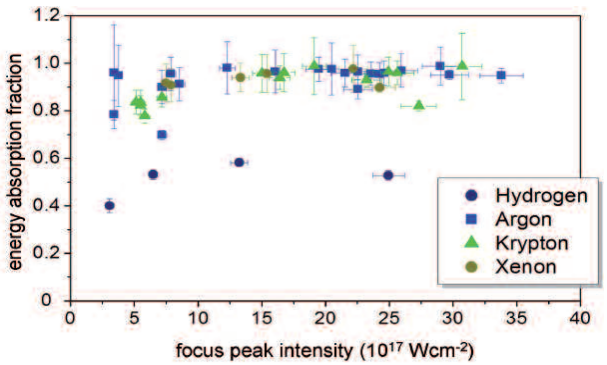

Figure 2. Absorption efficiency in different target gases. The Absorption exceeds 80% for most shots, except for H_2 where it only reaches about 50% over the full measured range.

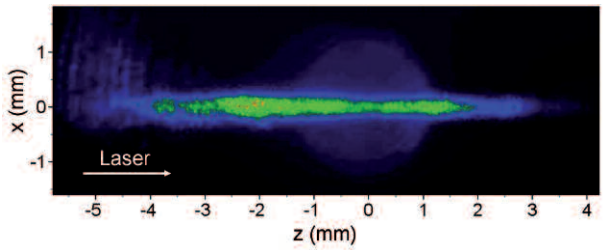

Figure 3. False-colour image of the absorption volume in Kr illuminated with 10 J. The outline of the nozzle is visible to the right of the image centre as a brighter circular area. The laser is coming in from the left and focuses at x = z = 0.

the measurements published in ref. [6], where H_2 also exhibited 90% absorption when irradiated with 10^{17} Wcm^{-2}. However, the previous measurement was done with a larger average cluster size (10 nm), which could explain the lower absorption, given the relatively long 1.3 ps heating pulse. This however can only be fully addressed with detailed simulations which would go beyond the scope of this report.

A false-colour image of the absorption volume, as recorded by a visible Andor camera (DV420), is shown in figure 3. The emission was not spectrally resolved, making it difficult to explain the exact physical origin. However, the overall shape of the imaged volume is comparable to the beam profile as it focuses above the nozzle. Furthermore, the emission is relatively uniform indicating it is not driven by a non-linear process such as Raman scattering. This suggests that the imaged radiation is dominated by visible plasma self-emission emitted during the strong cluster heating early on (~ps) in the interaction. Therefore the image should give information about the volume of energy deposition.

Notably, there is substantial energy deposition over a range of several Rayleigh lengths ($z_R \approx 1$ mm) on either side of the focus, which is centred above the nozzle at z = 0. The bright area of the imaged plasma typically has a volume of ~0.5 mm^3 which allows to estimate the energy density in the plasma to be as high as ~10^5 Jcm^{-3} (~3×10^9 Jg^{-1} for H_2). It can clearly be seen that the energy deposition starts well before the point of best focus, posing the question whether the beam actually reaches the peak intensities as calculated via the pulse energy and focal spot size. Nevertheless, substantial self-emission observed after the focal position indicates that even for z > 0 sufficient energy remains to drive significant cluster heating.

Energy transport and shock evolution

The energy deposition by the laser into the cluster medium results in substantial heating of the plasma and subsequent energy transport away from the initial interaction region in the form of a shock. The shock evolution was measured with optical probing, providing spatially resolved Schlieren and interferometry snapshots, as well as a streaked Schlieren diagnostic giving a full temporal evolution of the system.

An example of the data is displayed in figure 4. It shows a Schlieren and interferometry image of H_2 after 2.6 ns as

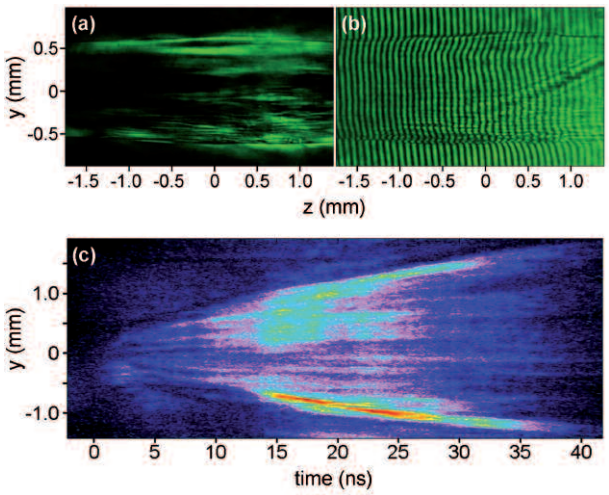

Figure 4. Example of shock data. (a) shows a 2D time framed Schlieren image and (b) an interferometry image from the same shock in H_2 taken after 2.6 ns, (c) is the full streaked shock evolution imaging only a 1D slice of the shock. In all images, y = z = 0 denotes the laser focus position.

well as a streaked image of the shot. The shock front can clearly be seen in all images. The region displayed in figure 4(a) and (b) corresponds to an absorption length of ~3.5 mm confirming that energy is deposited over a significantly longer distance than the Rayleigh length z_R. One of the major advantages of the streaked Schlieren diagnostic is the ability to extract the full blast wave evolution from a single shot rather than having to rely on several snapshots and repeatability of the experimental parameters. Some early results from this diagnostic are presented in figure 5 along with a trajectory obtained from fitting a power law to the shock front relating the blast wave trajectory r(t) to the deposited energy E and the time t.

$$r(E,t) \sim E^{\alpha/2}\, t^{\alpha} \qquad (1)$$

Here, α is called the *deceleration parameter*.

At early times, the expansion velocity exceeds 10^7 cms^{-1} in all gases, but rapidly slows down ($\alpha < 1$) accompanied by a drastic cooling of the plasma from several keV to a few eV.

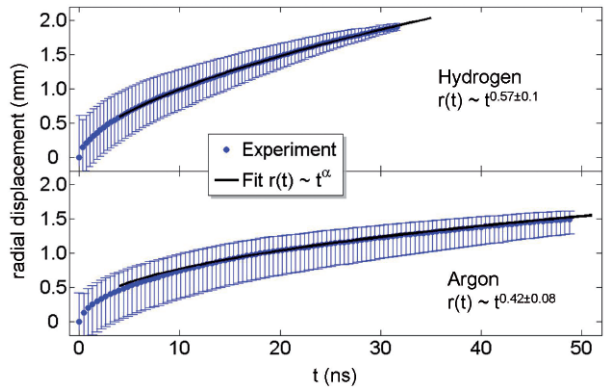

Figure 5. Blast wave trajectories extracted from streaked Schlieren data. The data is fitted with a power law function, which indicates a slightly faster expansion in H_2 than expected from theoretical predictions.

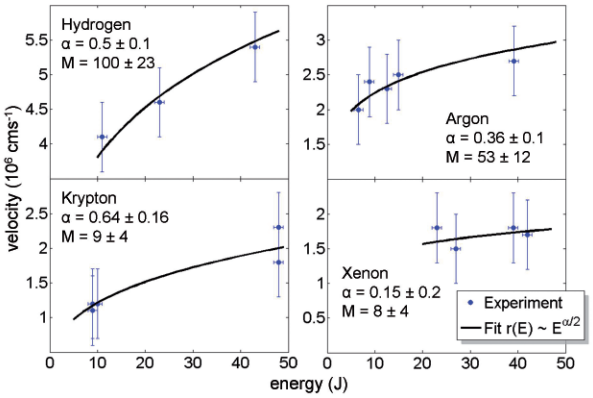

Figure 6. Shock velocity as a function of deposited energy for H_2, Ar, Kr and Xe clusters. The small number of data points limits the accuracy of the fitted function significantly. Nevertheless it is clear that Kr departs significantly from the results obtained with the other gases.

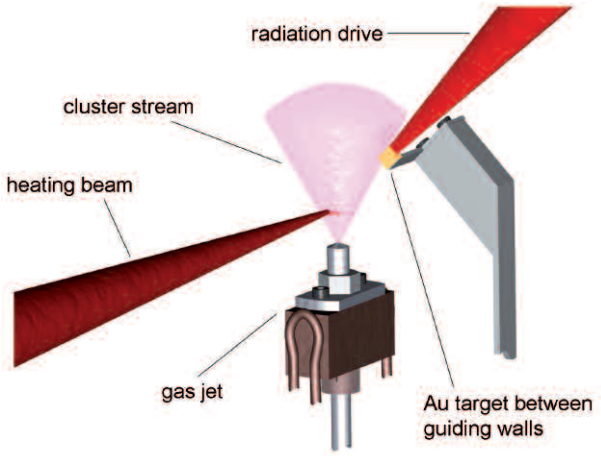

Figure 7. Schematic drawing of the radiation drive setup.

For H_2 energy losses through radiation are negligible, and the blast wave evolution is expected to follow the theoretical energy-conserving Sedov-Taylor solution with $\alpha = {}^1/_2$ (for cylindrical geometry). For higher Z gases the cooling is dominated by radiation which causes a radiative precursor ahead of the shock. The precursor is driven by radiation emitted from the shock that is re-absorbed in the upstream gas which then becomes ionised. This heat loss causes an increased deceleration meaning that α should decrease with increasing Z. This is observed in the experimental data with H_2 following a trajectory consistent with the Sedov-Taylor value within experimental uncertainty and Ar exhibiting a faster deceleration.

In the same way, one can plot the expansion velocity for each gas as a function of the energy according to equation (1). We performed a series of measurements for the four gases at a range of laser energies, which are presented in figure 6 along with the equivalent power law fit. In this first experiment, a complete set of streaked Schlieren data was not acquired for all gases and laser energies of interest. Thus in some cases the velocities are extracted from time framed data and are averaged over a time interval (~5 ns to ~25 ns) consequently resulting in error bars larger than for the streaked Schlieren data. Figure 6 also contains Mach numbers M for the shock expansion calculated for the fastest observed shock velocity in each gas. To estimate M the upstream temperature ahead of the shock front has to be taken into account. Consequently the Mach number is largest for H_2 with M = 100 ± 23, since the shock velocity is highest and the upstream gas is not heated by radiative losses from the shock.

In these data, H_2 is consistent with the theoretical Sedov-Taylor prediction of $\alpha = {}^1/_2$ for cylindrical geometry, whilst Ar and Xe decelerate faster, as expected. Although the available data for Kr is very limited, it does suggest that $\alpha > {}^1/_2$. A deceleration parameter exceeding $^1/_2$ can occur during a period in the evolution of a blast wave when it gains energy by sweeping up the pre-heated upstream gas. This energy-recovery phase has been observed in previous studies [5] but requires detailed trajectory information to quantify.

Radiative pre-heat

An important difference between many astrophysical systems compared to laboratory experiments is the presence of the interstellar medium and a degree of background ionisation. Whereas astrophysical phenomena such as SNRs typically interact with weakly ionised gas, the ambient medium in laboratory-scale systems will generally be cold and neutral. At this point it is unclear how this affects the experimental outcome and how big the impact on the hydrodynamics is, that describe the system. We have performed experiments to investigate this aspect.

Radiation drive targets were designed using the radiation-hydrodynamics code HELIOS [9] and aimed to deliver a directed ~50 eV X-ray flux when illuminated with a long pulse beam (5 ns, 150 J). The 20 µm Au foil used to produce X-rays via laser heating was mounted at one end of a parallel pair of Au coated glass plates in order to collect and guide soft X-rays. A schematic drawing of the setup is shown in figure 7.

An example shot with radiation drive is displayed in figure 8. The dark rectangular area at the top right is a shadow of the radiation target mount. The main shock, expanding in the horizontal plane, has evolved for 25.4 ns. The radiation drive beam, coming from the top in figure 8, impacts on the radiation target 4.5 ns after the initial interaction. This results in a radiation fan covering a vertical slice of the target gas underneath the foil (denoted by the blue dashed lines in figure 8). The foil itself survives long enough to completely shield the drive laser, preventing it from interacting with the gas target directly.

The effect of the radiation is clearly seen in the image centre, where a secondary shock is launched in the vertical plane on top of the primary shock. There is only very little indication of the X-ray drive outside the primary shock, other than a slight modulation on the shock front and a minor acceleration in the area covered by the radiation. It should be noted however, that this target geometry could be further improved, as the radiation interacts with an entire target medium crossection including both shocked and unshocked material. Ideally, the radiation would only impact material ahead of the shock so that a change in

shock dynamics can only be attributed to the interaction with ionised material rather than the radiation impact on the shock itself. However, from the result it is safe to assume, the radiation drive does have an impact. The specifics of this particular change in shock dynamics will have to be determined with a modified target geometry in future experiments.

Conclusions

In conclusion, we have conducted detailed measurements that significantly extend previous research concerning absorption of high-intensity laser radiation by atomic clusters, and used the resulting plasmas to investigate shock propagation under extreme conditons. The results show clusters efficiently absorb laser light spanning at least four orders of magnitude in intensity and three orders of magnitude in energy.

Investigations of shock propagation have resulted in extensive data of blast wave trajectories and time and space evolution for a variety of target gases and experimental parameters. Sedov-Taylor blast waves were observed in H_2 with Mach numbers as high as ~100. Blast waves in Ar and Xe exhibited radiative energy loss as evidenced by reduced deceleration parameters measured through the blast wave trajectory and the scaling of shock velocity with laser energy. A deceleration parameter in Kr exceeding the energy-conserving value of $\alpha = {}^1/_2$ suggests that in this case some energy is recovered from the heated upstream gas as the blast wave propagates.

Finally, we have conducted the first ever measurement of the impact of the target medium ionisation state on the shock dynamics. Preliminary results indicate the heated upstream medium results in shock acceleration but to clarify the results, the experiment will have to be revisited with a modified geometry.

Acknowledgements

The authors gratefully acknowledge the support by the operational staff of the Central Laser Facility and technical support from P. Ruthven and B. Ratnasekara of Imperial College. This work was supported by the UK Engineering and Physical Sciences Research Council (EPSRC).

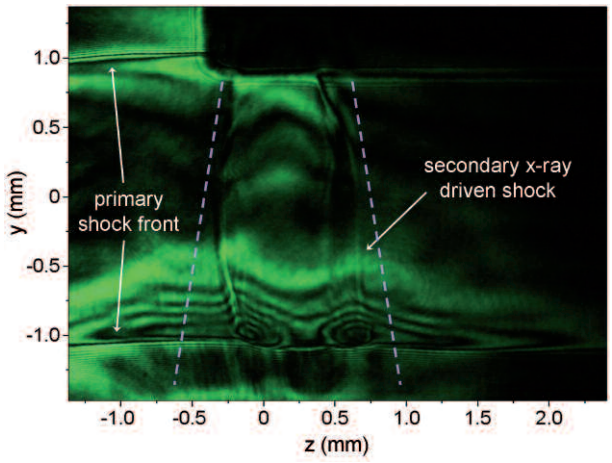

Figure 8. Radiation drive incident on a shock in Ar after 25.4 ns. The impact of radiation is mainly visible in the primary shock in the form of a secondary shock in the vertical plane. The blue dashed lines denote the area approximately covered by the X-ray drive.

References

1. B. A. Remington *et al.*, *Science* **284**, 1488-1493 (1999).
2. B. A. Remington, R. P. Drake and D. D. Ryutov, *Rev. Mod. Phys.* **78**, 755 (2006).
3. D. D. Ryutov *et al.*, *Astrophys. J.* **518**, 821-832 (1999).
4. D. N. Burrows *et al.*, *Astrophys. J.* **543**, L149-L152 (2000).
5. M. J. Edwards *et al.*, *Phys. Rev. Lett.* **87**, 085004 (2001).
6. A. S. Moore, D. R. Symes and R. A. Smith, *Phys. Plasmas* **12**, 052707 (2005).
7. D. R. Symes *et al.*, *High Energy Density Physics* **3**, 353 (2007).
8. A. S. Moore *et al.*, *Phys. Rev. Lett.* **100**, 055001 (2008).
9. T. Ditmire *et al.*, *Phys. Rev. Lett.* **78**, 3121 (1997).
10. J. Lazarus *et al.*, CLF Annual Report 2004/2005, page 40.
11. E. T. Gumbrell *et al.*, submitted to *New J. Phys*.
12. A. S. Moore *et al.*, CLF Annual Report 2004/2005, page 34.
13. MacFarlane *et al.*, *J. Quant. Spectrosc. Rad. Transfer* **99**, 381 (2006).